

Structural Geology
and
Personal Computers

Structural Geology
and
Personal Computers

Edited by

Declan G De Paor
Department of Earth and Planetary Sciences
Harvard University



Pergamon

U.K.	Elsevier Science Ltd, The Boulevard, Langford Lane, Kidlington, Oxford OX5 1GB, U.K.
U.S.A.	Elsevier Science Inc., 660 White Plains Road, Tarrytown, New York 10591-5153. U.S.A.
JAPAN	Elsevier Science Japan, Tsunashima Building Annex, 3-20-12 Yushima, Bunkyo-ku, Tokyo 113, Japan

Copyright ©1996 Elsevier Science Ltd

All Rights Reserved. No part of this publication may be reproduced, stored in a retrieval system or transmitted in any form or by any means electronic, electrostatic, magnetic tape, mechanical, photocopying, recording or otherwise, without permission in writing from the publishers.

First edition 1996

Library of Congress Cataloging in Publication Data

A catalog record for this book is available from the Library of Congress.

British Library Cataloguing in Publication Data

Structural geology and personal computers. – (Computer methods in the geosciences; v. 15)

1. Geology, Structural – Data processing

I. De Paor, Declan G.

551.8'0285

ISBN 0 08 042430 9 (cased version)

ISBN 0 08 043110 0 (flexi version)

Calculation of Rock Properties from Pole Figures Using *LabView*

Johann Lapierre, David Mainprice, and Walid Ben Ismail

Laboratoire de Tectonophysique, Université Montpellier II, Place E.
Bataillon, 34095 Montpellier cédex 05, France. johann@dstu.univ-montp2.fr
david@dstu.univ-montp2.fr walid@dstu.univ-montp2.fr

Abstract—Calculating physical properties of rocks requires an Orientation Distribution Function (ODF) of crystalline aggregates derived from individual orientation data (*i.e.*, in general, universal stage measurements). Though frequently projected and contoured on stereograms to yield pole figures for tectonic interpretations, orientation datasets are rarely published and are often lost. To calculate physical properties, we developed an image processing method to recover orientation density data from published pole figures. An inversion program used in materials science was modified to derive partial ODFs from recovered orientation density dataset. We describe the full method implemented in the *LabView*TM program *SCANSTEREO* for orientation density recovery and in the *FORTTRAN77*TM program *INVPOLE* for ODF calculation. We give a test of consistency between seismic properties derived from inverted and measured data for a peridotite sample from Lanzo massif (Alps, Italy).

Introduction

Many rock-forming minerals are intrinsically anisotropic as single crystals, and aggregates often contain an anisotropic distribution of crystals. This leads to the concept of rock texture (commonly called petrofabric) which may be mathematically described by the orientation distribution function (ODF). An ODF is the essential parameter to determine physical properties of anisotropic rocks (*e.g.*, Mainprice *et al.* 1993, Mainprice & Humbert 1994) and is critical for the interpretation of geophysical data such as seismic anisotropy or electric and thermal properties.

Petrofabrics have been used classically as indicators of shear sense on rocks deformed at *P/T* conditions permitting plastic behaviour (Nicolas *et al.* 1973, Schmidt & Casey 1986); they are now being used increasingly to calculate rock physical properties. Recent studies of teleseismic shear-wave splitting (Mainprice & Silver 1993, Barruol & Mainprice 1993) have shown that relationships between petrofabric and anisotropic seismic properties allow the determination of the directions of plastic flow in the upper mantle. Furthermore, a

classification of mantle textures and related seismic anisotropy has been initiated (Ben Ismail 1995) on the basis of 110 measured petrofabrics from various geodynamical contexts. Elastic properties of crustal rocks derived from petrofabrics are also useful to characterize seismic reflectors detected during deep continental seismic reflection profiling (*e.g.*, COCORP, ECORS, DECORP, *etc.*).

The above studies are restricted to a small number of petrofabrics and the desirability of establishing a more comprehensive database is clear. Such a revival of interest in texture analysis has prompted the acquisition of new data sets as well as the use of existing ones. However, the problem of retrieving lost data sets from petrofabric projections such as pole figures has not been addressed. For example, numerous existing petrofabric data were stored on IBM punch cards, but almost complete obsolescence of such data storage methods means the majority of this data has been lost. Moreover, original petrofabric data sets related to published pole figures are often unavailable in the literature (*e.g.*, in theses). We solve this problem by introducing a method combining image processing and numerical techniques derived from texture goniometry to recover the ODF from published pole figures.

We review the main features of pole figures to show which types of data are recoverable. Then we present an image processing procedure (*SCANSTEREO*) to extract point orientation density values from digitized images of pole figures. Next, we explain briefly the inversion procedure (*INVPOLE*) which allows the calculation of the ODF coefficients on the basis of data provided by *SCANSTEREO*. Finally, we develop an application on a known peridotite sample from Lanzo massif (Alps, Italy) to compare seismic properties derived from original and inverted datasets in order to estimate the bias introduced by the inversion method.

The Pole Figure Geometry and Its Implications

A pole figure is a representation of the Lattice Preferred Orientations (LPO) of a rock-forming mineral population (see Nicolas & Poirier 1976 for a review). Typically, it is plotted as a scatter diagram on lower hemisphere equal area projection. Individual orientation data as derived from universal stage measurements are a population of individual poles. The data are contoured to obtain an orientation density diagram. Data derived from volume diffraction measurements (*e.g.*, X-ray or neutron texture goniometry) are routinely presented as contoured diagrams. A pole figure can be defined analytically by the density of crystallographic orientation $P_{(h)}(y)$ in a y direction of the structural reference frame, and describes the fundamental relationship of texture:

$$P_{h_i}(y) = \frac{1}{2\Pi_{h_i//y}} \int f(g) d\chi \quad (1)$$

with:

h_i : A crystallographic direction corresponding to the normal to a low-index lattice plane with Miller indices h_1, h_2, h_3 .

$f(g)$: The ODF which may be defined in terms of generalized spherical harmonics (Bunge 1982).

$d\chi$: An element of solid angle in the unit hemisphere of the projection.

In practice, orientation density counting is often achieved using the Schmidt grid on the projected data set. Counting and contouring methods are many (*e.g.*, Vollmer 1995 for a recent review) but, essentially, they all smooth and interpolate the individual poles. Thus, it is impossible to recover the original data set of individual measurements from the pole figure and the only alternative is to produce a lower accuracy gridded set for given increments in azimuth and inclination such as those used in contouring texture goniometry measurements. This is detailed in the two next sections where we describe how digitized images of pole figures are processed. A first pre-processing stage is necessary to preserve only orientation density information and to convert density areas into an appropriate format. Then pole figure center coordinates and radius are calculated to produce a circular grid in order to extract grayscale density values.

Setting Up the Image of the Pole Figure

The images of pole figures are digitized with a flat-bed scanner and saved as TIFF 256 gray level images. Objects not related to density information (labels, scanning noise, *etc.*) are removed from the images. Because the pole figures considered here are contour plots, we need to produce an image with homogeneous gray level areas corresponding to each different density interval. We have done this with Adobe *Photoshop*[™] 2.5.1, but it can be achieved with any drawing software. It is simply necessary to join the contour lines delimiting the density areas, and then fill them with a gray level representing the density value. The gray level scale can be chosen arbitrarily within the range of 1 to 254 gray value. The values 0 and 255 are reserved for diagram background and zero density areas respectively. After these operations the image can be processed with the *SCANSTEREO* program.

Working Procedure of the Program *SCANSTEREO*

Reading the Image

SCANSTEREO reads uncompressed 256 gray level TIFF or PICT images. The user can choose between processing only one image or a folder (directory) of images which are all identically grayscaled. In the first case the image is displayed full size if the resolution is less than 300×300 pixels, otherwise it is reduced to 300×300 pixels and displayed. In the folder option only the first image is displayed to save time and memory.

Processing the Image

SCANSTEREO first calculates the center coordinates and the radius of the pole figure as follows. The image is first thresholded in order to obtain a binary image

of the whole pole figure: levels between 1 and 255 are replaced by the value 1 and background remains as 0. Then the center coordinates of the diagram and the size of the rectangle which surrounds the pole figure are calculated. The diameter of the pole figure is obtained considering only the minimum of either the height or the width of the surrounding rectangle so that the scanned data points are as much as possible contained within the pole figure even if its scanned image is not perfectly circular.

Next a sub-routine called *GREYDENS* allows the user to select the density value corresponding to each gray level automatically selected by the program. Then the *CALCGRID* subroutine scans the image assuming the pole figure to be an equal area projection and using a grid calculated with the following formulas:

$$X_{G_i} = \text{INT}(X_c + 2\sin(INC_i/2) \sin(AZ_i) R/\sqrt{2})$$
$$Y_{G_i} = \text{INT}(Y_c + 2\sin(INC_i/2) \cos(AZ_i) R/\sqrt{2})$$

where X_{G_i} and Y_{G_i} are the coordinates of the grid points (in pixels), X_C and Y_C are the center coordinates of the pole figure (in pixels), R is the radius of the pole figure (in pixels), INC_i is the inclination (from 0° to 90° every 5°) and AZ_i is the azimuth (from 0° to 355° every 5°). Note: as in most images and screen formats, the origin is in the top left hand corner.

For each point, X_{G_i} , Y_{G_i} , the gray level is extracted and the corresponding density value is stored in a 2D array. In order to avoid measuring points outside the diagram, when the inclination reaches 90° the *CALCGRID* subroutine checks if each point has a gray level of zero (*i.e.*, the point is outside of the pole figure). If this is true, it decreases the radius and recalculates the coordinates of the measured point until its gray value becomes different from zero. Finally the image is displayed full size with the grid superimposed.

Output of Results

The program *SCANSTEREO* produces a matrix of 19 rows by 72 columns containing the crystallographic orientation density values of the pole figure in an ASCII spreadsheet format file. Such a dataset is analogous to those obtained from X-ray or neutron goniometry. Consequently, a partial ODF may be calculated according to the inversion method implemented in the *INVPOLE* program, presented in the following section.

The Inversion Method

Inversion of pole figures has been widely developed in materials science (Bunge 1982) for X-ray or neutron goniometry. Recent work (Bunge & Wenk 1977, Casey 1981, Wagner & Humbert 1987) introduced inversion methods for the low symmetry materials which prevail in Earth sciences. These procedures make use of harmonic methods which lead to a spherical harmonic form of the ODF. We

Calculation of Rock Properties

outline only the principles of the inversions here; further details of the theory and formalization can be found in the above references.

The discrete development of the relation in eqn. (1) in terms of symmetrical generalized spherical harmonics may be expressed as follows:

$$P_{h_i}(y) = \sum_{l=0}^{\infty} \sum_{v=1}^{N(l)} F_l^v(h_i) k_l^v(y)$$

where $N(l)$ is the number of specimen symmetry harmonics, $k_l^v(y)$ are the spherical harmonics satisfying sample symmetry, and $F_l^v(h_i)$ denotes the theoretical coefficients of the pole figure which are related to the coefficients $C_l^{\mu\nu}$ of the serial development of the ODF:

$${}^{Th}F_l^v(h_i) = \frac{4\pi}{2l+1} \sum_{\mu=1}^{M(l)} C_l^{\mu\nu} k_l^{*\mu}(h_i) \quad (2)$$

Here, $M(l)$ is the number of linearly independent harmonics (*i.e.*, the number of independent measured pole figures), and $k_l^{*\mu}(h_i)$ are complex conjugates of spherical harmonics satisfying crystal symmetry. The coefficients $F_l^v(h_i)$ can also be related to measured pole density values $P_{h_i}(y)$ by:

$${}^{Meas}F_l^m(h_i) = \int_{\alpha=0}^{\pi/2} \int_{\beta=0}^{2\pi} P_{h_i}(y) k_l^{*v}(y) \sin\alpha d\alpha d\beta$$

where α and β are the spherical coordinates in the pole figure reference frame. Using eqns. (2) and (3) it is possible, for a given set of pole figures, to calculate the ODF coefficients $C_l^{\mu\nu}$ using a least square method:

$$\sum [{}^{Meas}F_l^m(h_i) - {}^{Th}F_l^v(h_i)]^2 = \min.$$

In the examples presented here, petrofabrics are derived from an individual measurement technique, the universal stage, hence the consistency of data between different pole figures of the same sample is better than those obtained by X-ray analysis. Therefore, we can expect a more accurate inversion.

Universal stage measurements that are used here are for olivine and are non-vectorial, that is directions are measured without a positive and negative sense, therefore pole figures are centrosymmetric. Hence the inversion method only permits the determination of the coefficients of the ODF for even values of l (expansion range of the spherical harmonics).

Relationships between $M(l)$ and l (equation (2)), depending on crystal symmetry given by Bunge (1982) and Humbert & Diz (1991), show that it is

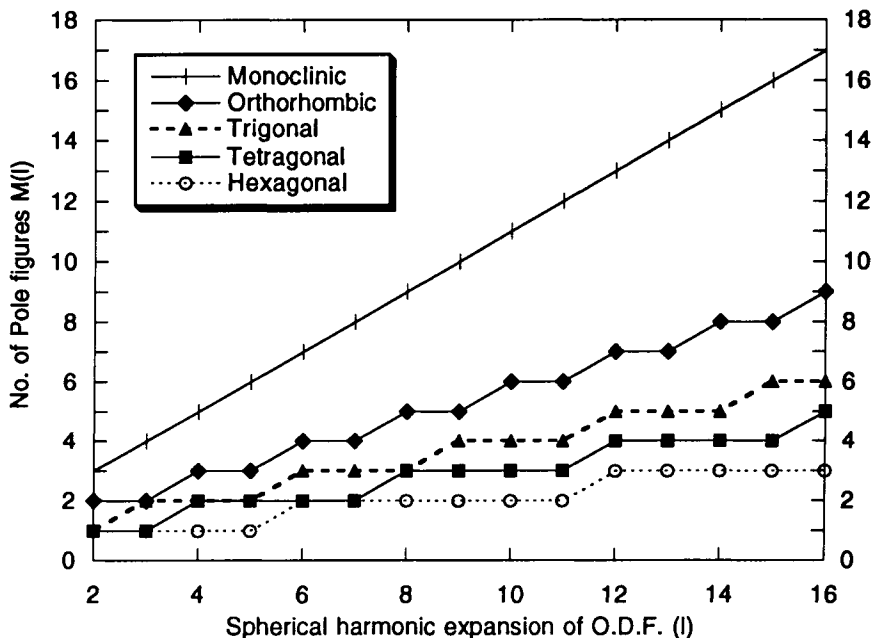


Fig. 1. Number of measured pole figures $M(l)$ required to reach given spherical harmonic expansion l of orientation distribution function for the crystal symmetries treated by program *INVPOLE*. For seismic properties $l = 4$ expansion is minimum requirement and therefore 1, 2, 2, 3, and 5 pole figures would be needed for hexagonal, tetragonal, trigonal, orthorhombic, and monoclinic crystal and triclinic specimen symmetries. Spherical harmonic expansions of 10 to 16 are typical for quantitative studies of lattice preferred orientation (texture) where many pole figures are required for low symmetry minerals.

possible to calculate physical properties of symmetrical tensors of orders 2 and 4 from ODFs characterized by spherical harmonics with $l = 2$ and $l = 4$, respectively. Because tensors related to physical properties of geophysical interest are centrosymmetric, the bias introduced by the centrosymmetry of the pole figure does not affect the present analysis.

The method of pole figure inversion can be applied to any crystal symmetry (Bunge 1982). In the present application two factors restrict its application, firstly the number of pole figures available, and secondly the numerical inversion scheme used. Published LPO are typically given for only three principal crystallographic directions in the structural reference frame (*i.e.*, three pole figures). This constitutes a limitation for the inversion method because Bunge (1982) showed that with lowering symmetry class (*i.e.* cubic towards triclinic) the number of independent pole figures required increases. For example, for hexagonal, tetragonal, trigonal, orthorhombic and monoclinic symmetry classes one requires 1, 2, 2, 3, and 5 independent pole figures, respectively, to calculate an ODF of order 4 for seismic properties. If only three independent pole figures ($M(l) = 3$) are published, tensors

Calculation of Rock Properties

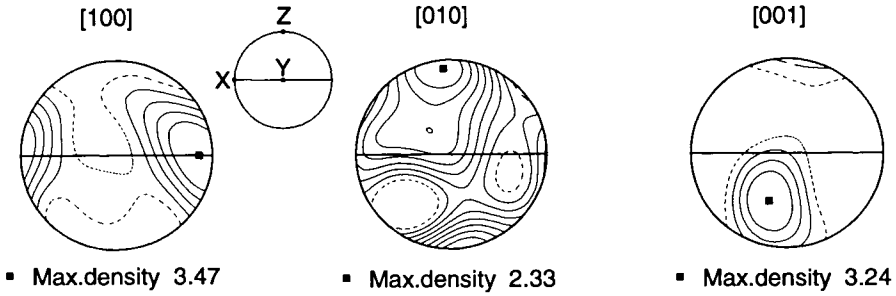


Fig. 2. Olivine pole figures of lherzolite for [100], [010], and [001]. Equal-area projection, lineation (X) east-west, foliation plane (XY) perpendicular to projection plane. Contour intervals 0.5 times uniform distribution for [100] and [001], 0.25 times for [010]; lowest contour is dashed line, higher values - solid lines. Highest value - black square.

of orders 2 and 4 (electric, thermal, and seismic properties) cannot be calculated for monoclinic or lower symmetry minerals (see Fig. 1). In the current application we have used the *INVPOLE* program developed in *FORTRAN 77* by Wagner & Humbert (1986). To make the inversion scheme as memory efficient as possible, this program is restricted to non-cubic crystal classes containing a two fold axis, hence excluding cubic and triclinic classes as shown in Fig. 1.

Calculation of Seismic Properties

To calculate the seismic properties of a polycrystal, one needs to evaluate the elastic properties of the aggregate. In the case of an aggregate with a crystallographic fabric or texture, the anisotropy of the elastic properties of the single crystal must be taken into account. For each orientation \mathbf{g} the single crystal properties have to be rotated into the specimen coordinate frame using the orientation matrix g_{ij} ,

$$C_{ijkl}(\mathbf{g}) = g_{im} g_{jn} g_{ko} g_{lp} C_{mnop}(\mathbf{g}^0)$$

where $C_{ijkl}(\mathbf{g})$ is the elastic property in sample coordinates, $\mathbf{g} = g_{ij} = g(\varphi_1 \phi \varphi_2)$ the measured orientation in sample coordinates and $C_{mnop}(\mathbf{g}^0)$ is the elastic property in crystal coordinates, with $\mathbf{g}^0 = g^0_{ij} = g^0(\varphi_1=0 \phi=0 \varphi_2=0)$.

The elastic properties of the polycrystal may be calculated by integration over all possible orientations of the ODF. The ODF may be derived from individual measurements and pole figure inversion as in the current application. Bunge (1982) has shown that integration is given as:

$$\langle C_{ijkl} \rangle = \int C_{ijkl}(\mathbf{g}) \cdot f(\mathbf{g}) d\mathbf{g}$$

where $\langle C_{ijkl} \rangle$ is the elastic tensor of the aggregate and $d\mathbf{g} = 1/8p^2 \sin\phi d\varphi_1 d\phi d\varphi_2$. The final step is the calculation of the three seismic phase velocities from the solution of the Christoffel equation:

$$\text{Det} \left| \langle C_{ijkl} \rangle X_i X_j - \delta_{ik} \rho V^2 \right| = 0$$

where $X_i X_j$ are the direction cosines of the wave propagation direction, ρ is density, δ_{ik} is the Kronecker delta, and V is one of the three seismic phase velocities. The calculation is repeated for every propagation direction on a hemisphere in 6 degree intervals and contoured (e.g., Fig. 2). The Voigt average has been used in all calculations presented here (see Mainprice & Humbert 1994 for further details).

Example

In order to validate results of the inversion method we compared seismic properties calculated after inversion of the pole figure and those derived from universal stage measurements. We could have presented the intermediate step by comparing the ODF calculated from the universal stage measurements and from the inverted pole figures at an expansion of order 4, but we chose to illustrate the method with calculated physical properties as this was the objective of our study. We used data from Boudier (1969), collected on a lherzolite sample from Lanzo massif (see Fig. 2 for related pole figures). We calculated the seismic properties of olivine because it is orthorhombic and therefore amenable to our method, which cannot be used for monoclinic and triclinic minerals. Contoured projections of P -wave velocities (V_p) presented in Figs. 3a and 3b show the same velocity distribution with a maximum close to the lineation (X), and a minimum perpendicular to the foliation plane (XY). Such coherence between the two methods of calculation is also qualitatively verified for projection of S -wave birefringence (dVs) and fastest S -wave polarization plane displayed in Figs. 3d, 3e, 3g, and 3h, respectively. Quantitatively, the errors on P -wave velocity and S -wave birefringence for the principal directions of the structural reference frame are summarized in Table 1, which shows only values less than 1%. These errors have also been projected and contoured on pole figures displayed in Fig. 3c for V_p and Fig. 3f for dVs . Both stereograms show a minimum close to the foliation plane and perpendicular to the lineation related to the *SCANSTEREO* grid resolution which is more important in the center of the pole figure. Generally, the distributions of these errors are related to a combination of the lack of accuracy of the *SCANSTEREO* scanning circular grid and the smoothing and interpolation necessary to construct the original pole figure.

Conclusion

Although this inversion method does not provide optimal determination of the ODF, it allows satisfying calculations of seismic properties. Qualitatively the results are very similar to those derived from original measurements. Quantitatively, V_p and dVs determination is very accurate in all directions of the structural reference frame (generally, error is less than 5%). As a result, orientation distribution of seismic anisotropy in the structural reference frame may be derived from the published pole figures without individual lattice orientation measurements. This method will allow the establishment of an interpretive

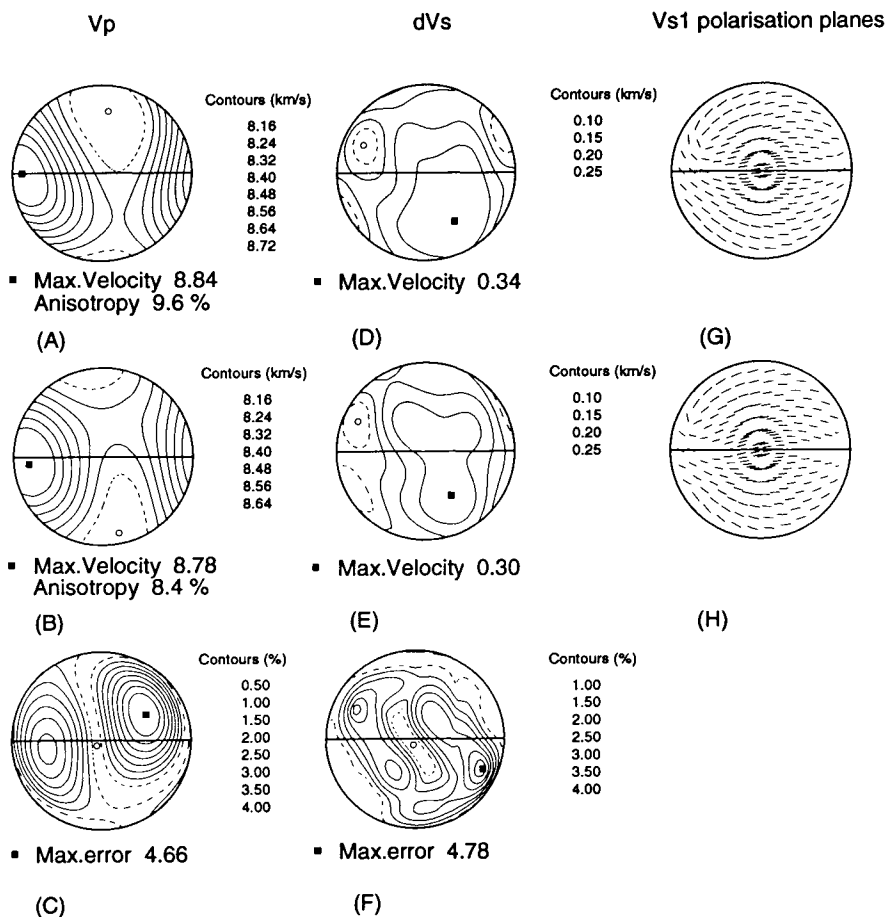


Fig. 3. Seismic properties of lherzolite sample with olivine calculated directly and after inversion, and related errors. Maximum values – black square, minimum values – open circle. a) Contoured P -wave distribution calculated from individual measurements (km/s). b) Contoured P -wave distribution calculated from recovered data (km/s). c) Contoured P -wave error on V_p estimate (%). d) Contoured S -wave birefringence distribution calculated from individual measurements (km/s). e) Contoured S -wave birefringence distribution calculated from recovered data (km/s). f) Contoured error on dV_s estimate (%). g) Fastest S -wave polarization plane derived from individual measurements. h) Fastest S -wave polarization plane derived from recovered data.

Table 1. Seismic wave velocities and birefringence and related errors in the principal directions of the structural reference frame.

Azimuth / Inclination	0°/90° Y	0°/0° Z	90°/0° X
Vp direct (km/s)	8.104	8.203	8.796
Vp inv. (km/s)	8.100	8.244	8.722
Vp error	0.5%	0.049%	0.84%
Vs1 direct (km/s)	4.820	4.879	4.913
Vs1 inv. (km/s)	4.798	4.912	4.886
Vs1 error	0.22%	0.23%	0.27%
Vs2 direct (km/s)	4.595	4.618	4.744
Vs2 inv. (km/s)	4.630	4.640	4.756
Vs2 error (km/s)	0.35%	0.22%	0.12%
dVs direct (km/s)	0.225	0.261	0.169
dVs inv. (km/s)	0.168	0.262	0.130
dVs error	0.57%	0.45%	0.39%

framework for teleseismic studies of the upper mantle, which consists mostly of orthorhombic minerals.

Acknowledgements

We thank G. Barruol, B. Ildefonse, R. M. Russo, and A. Wendt for useful discussion and review of this work. Special thanks go to F. Boudier who provided the original universal stage measurements as part of her Thesis in 1969. We would also like to thank F. Wagner (University of Metz) who provided a copy of *INVPOLE*. Finally we thank the reviewers for their helpful comments.

References

- Barruol, G. & Mainprice, D. 1993. A quantitative evaluation of the contribution of crustal rocks to shear-wave splitting of teleseismic SKS waves: *Phys. Earth Planet. Inter.* **78**: 281-300.
- Ben Ismail, W. 1995. *Variation de l'anisotropie sismique du manteau supérieur par l'étude de pétrofabriques d'olivine*. Rapport DEA: Université de Montpellier II, 47 pp.
- Boudier, F. 1969. *Le massif lherzolitique de Lanzo (Alpes Piemontaises) Etude structurale et pétrologique*. Thèse de doctorat: Université de Nantes, 163 pp.

Calculation of Rock Properties

- Bunge, H. J. & Wenk, H. R. 1977. Three-dimensional texture analysis of three quartzites (trigonal crystal and triclinic specimen symmetry): *Tectonophysics* **40**: 257-285.
- Bunge, H. J. 1982. *Texture analysis in materials science*. Butterworths, London, 593 pp.
- Casey, M. 1981. Numerical analysis of X-ray texture data: an implementation in *FORTTRAN* allowing triclinic or axial specimen symmetry and most crystal symmetries. *Tectonophysics* **78**: 51-64.
- Humbert, M. & Diz, J. 1991. Some practical features for calculating the polycrystalline elastic properties from texture. *J. Appl. Cryst.* **24**: 978-981.
- Mainprice, D. & Humbert, M. 1994. Methods of calculating petrophysical properties from lattice preferred orientation data. *Survey Geophys.* **15**: 575-592.
- Mainprice, D., Lloyd, G. E. & Casey, M. 1993. Individual orientation measurements in quartz polycrystals: advantages and limitations for texture and petrophysical property determinations. *J. Struct. Geol.* **15**: 1169-1187.
- Mainprice, D. & Silver, P. 1993. Interpretation of SKS-waves using samples from the subcontinental lithosphere. *Phys. Earth Planet. Inter.* **78**: 257-280.
- Nicolas, A., Boudier, F., & Boullier, A. M. 1971. Mechanisms of flow in naturally and experimentally deformed peridotites. *Am. J. Sci.* **273**: 853-876.
- Schmidt, S. M. & Casey, M., 1986. Complete fabric analysis of some commonly observed quartz *c*-axis patterns. In : H. C. Heard, H. C. & Hobbs, B. E. (eds.). Mineral and rock deformation: Laboratory studies-The Paterson volume. *AGU Monogr.* **36**. AGU, Washington, D.C., pp. 263-286.
- Vollmer, F. W. 1995. C program for automatic contouring of spherical orientation data using a modified Kamb method. *Comp & Geosci.* **21**: 31-49.
- Wagner, F. & Humbert, M. 1987. Texture analysis from incomplete pole figures in low symmetry cases: *Textures & Microstruct.* **7**: 115-129.

Appendix

SCANSTEREO Algorithm

Because *SCANSTEREO* has been implemented under *LabView* 3.0 with the *Concept™ VI* image analysis package which is copyright protected, we just give a C-like pseudo code easily adaptable in other programming environments (e.g., *NIH Image* macro). For those who own the licenses, the *LabView VI* is available by contacting D. Mainprice (david@dstu.univ-montp2.fr)

Structural Geology and Personal Computers

```

Read_Image (Original_Image);
Display (Image_Window_0, Original_Image);
Threshold_Image (Low_Limit=1, High_Limit=255, Replace_Value=1, Image_In=Original_Image, Image_Out=Thresholded_Image);
Get_Parameters (Image_In=Thresholded_Image, Center_X, Center_Y, Rectangle_Width, Rectangle_Height);
Diameter = Min (Rectangle_Width, Rectangle_Height);
Radius = Diameter/2;
Array_Histogram=Get_Image_Histogram (Original_Image);
For (i=1; i<256; i++)
|
|   {
|   |   Density[i]=0;
|   |   }
For (j=1; j<256; j++)
|
|   {
|   |   If (Array_Histogram[i] <> 0)
|   |   |   {
|   |   |   |   /* BEGINNING OF GREYDENS SUB-ROUTINE*/
|   |   |   |   Open_Image_Window (Image_Window_1);
|   |   |   |   j=0;
|   |   |   |   While (Get_Button_Value ('OK', Default_Value=FALSE) == FALSE)
|   |   |   |   |   {
|   |   |   |   |   |   If j==0;
|   |   |   |   |   |   |   Threshold_Image (Low_Limit=i, High_Limit=i,
|   |   |   |   |   |   |   |   Replace_Value=255-i, Image_In= Original_Image,
|   |   |   |   |   |   |   |   Image_Out= Thresholded_Image_1);
|   |   |   |   |   |   |   /*HIGHLIGHTS THE AREAS OF INTEREST */
|   |   |   |   |   |   |   If int(j/2)==j/2
|   |   |   |   |   |   |   |   Display (Image_Window_1, Original_Image);
|   |   |   |   |   |   |   |   else
|   |   |   |   |   |   |   |   |   Display (Image_Window_1, Thresholded_Image_1)
|   |   |   |   |   |   |   |   Density[i]=Get_Slider_Value ('DENSITY', Default_Value=
|   |   |   |   |   |   |   |   Density[i-1]);
|   |   |   |   |   |   |   |   j+=1;
|   |   |   |   |   |   |   |   }
|   |   |   |   |   |   |   Close_Image_Window (Image_Window_1);
|   |   |   |   |   |   |   /* END OF GREYDENS SUB-ROUTINE*/
|   |   |   |   |   |   }
|   |   }
|   }
/* BEGINNING OF CALCGRID SUB-ROUTINE*/
For (i=0; i<19; i++)
|
|   {
|   |   INC=i*5*3.14/180;
|   |   For (j=0; j<72; j++)
|   |   |   {
|   |   |   |   AZ=j*5*3.14/180;
|   |   |   |   While (temp=0)
|   |   |   |   |   {
|   |   |   |   |   |   Grid_X=Center_X+sin (INC/2)*sin (AZ)*Radius/SQRT(2);
|   |   |   |   |   |   Grid_Y=Center_Y-sin (INC/2)*cos (AZ)*Radius/SQRT(2);
|   |   |   |   |   |   temp=Get_Pixel_Value (Original_Image, Grid_X, Grid_Y);
|   |   |   |   |   |   /*AVOIDS MEASURING OUTSIDE OF THE POLE FIGURE*/
|   |   |   |   |   |   if i==18
|   |   |   |   |   |   |   {
|   |   |   |   |   |   |   |   if temp==0
|   |   |   |   |   |   |   |   |   Radius-=1;
|   |   |   |   |   |   |   |   else
|   |   |   |   |   |   |   |   |   {
|   |   |   |   |   |   |   |   |   |   Set_Pixel_Value (Original_Image, Grid_X,
|   |   |   |   |   |   |   |   |   |   Grid_Y, 255-temp);
|   |   |   |   |   |   |   |   |   |   Array_Out [i, j] = Density[temp];
|   |   |   |   |   |   |   |   |   |   }
|   |   |   |   |   |   |   |   }
|   |   |   |   |   |   |   |   else
|   |   |   |   |   |   |   |   |   {
|   |   |   |   |   |   |   |   |   |   Set_Pixel_Value (Original_Image, Grid_X, Grid_Y, 255-temp);
|   |   |   |   |   |   |   |   |   |   Array_Out [i, j] = Density[temp];
|   |   |   |   |   |   |   |   |   |   }
|   |   |   |   |   |   |   |   }
|   |   |   |   |   |   }
|   |   }
|   }
/* END OF CALCGRID SUB-ROUTINE*/
Display (Image_Window_0, Original_Image);
Write_To_File (Array_Out);

```